

Modélisation mathématique de certains aspects de la dégénérescence maculaire liée à l'âge (DMLA)

—

A modelling perspective on retinal (patho-)physiology

Luca Alasio

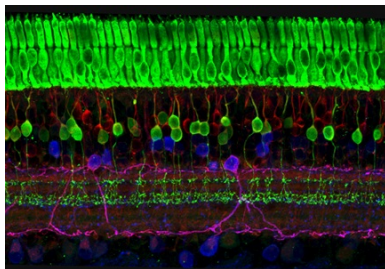
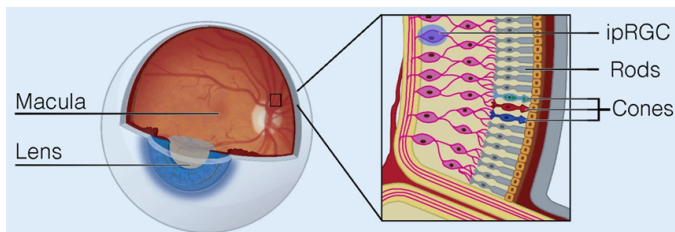


In collaboration with L. Almeida, Y. Borella, M. Paques, B. Perthame.

22/03/2024

Séminaire du LJLL

Structure of the retina



[Top] Blume et al., 2019 <https://doi.org/10.1007/s11818-019-00215-x>.

[Bottom] Wei Li, National Eye Institute, <https://www.flickr.com/photos/nihgov/>

Retinal degeneration

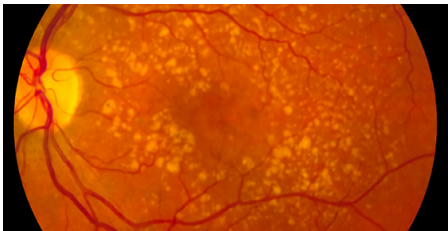
Dysfunctions of rods, cones and RPE are related to retinal degenerations.

Why is this urgent? - Age-related Macular Degeneration (AMD)

Public health issue: increasing projections of AMD patients worldwide,

- 196 million in 2020,
- 288 million in 2040. (Wong et al., The Lancet Global Health 2014)

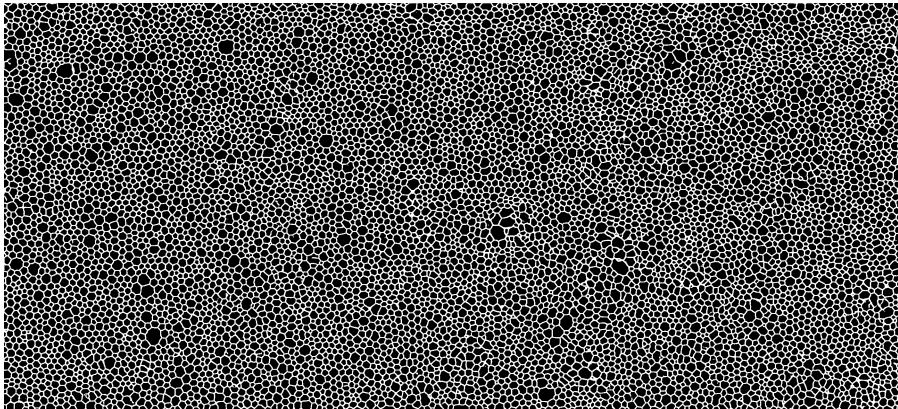
No treatment is currently available (for non-neovascular AMD).



A fundus photo showing intermediate age-related macular degeneration.

Credit: National Eye Institute, National Institutes of Health, Ref#: EDA2

Human RPE mosaic



Courtesy of Y. Borella, M. Darche, M. Paques, Paris Eye Imaging group, Hôpital Quinze-Vingts.

Mosaic changes due to ageing

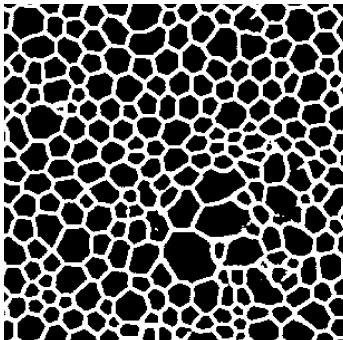
What is the expected behaviour of **ageing RPE** cells?

- no cell division, almost no migration;
- small gap closure, actin cable mechanism;
- senescence, size “relaxation”.

Mosaic changes in AMD, initial anomalies

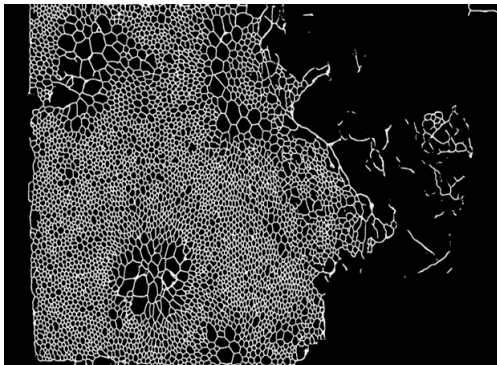
What happens as age-related macular degeneration progresses?

- drusen formation;
- hyper- and hypo- contracted cells;
- (eventually) tissue discontinuity.

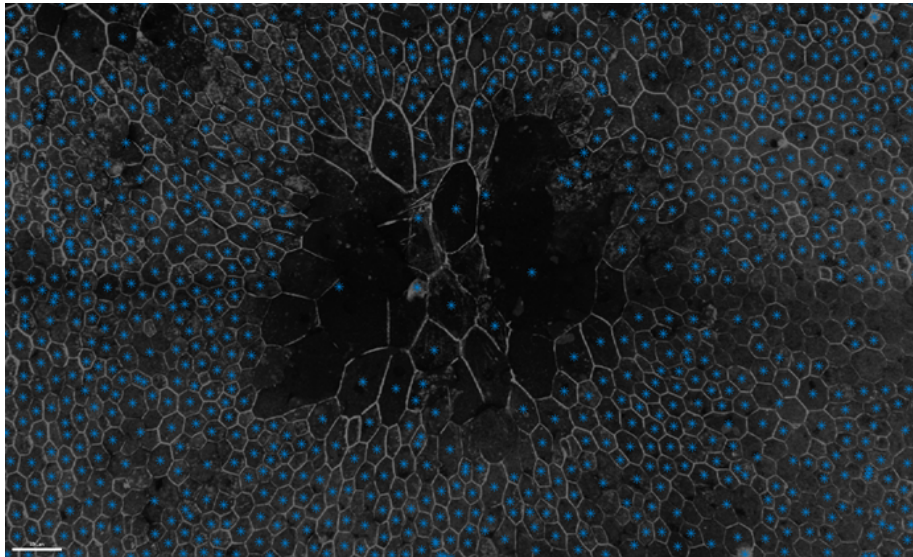


Courtesy of Y. Borella, M. Darche, M. Paques, Paris Eye Imaging group, Hôpital Quinze-Vingts.

Tissue discontinuity - large lesions



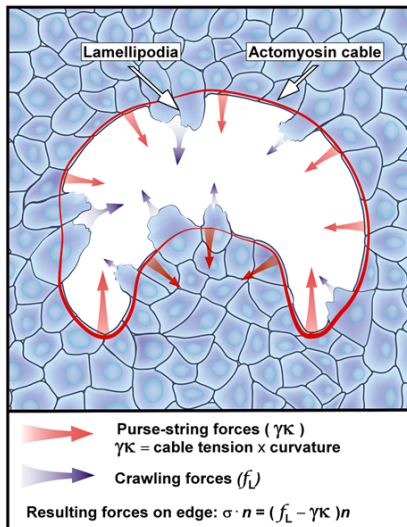
Courtesy of Y. Borella, M. Darche, M. Paques, Paris Eye Imaging group, Hôpital Quinze-Vingts.



Courtesy of Y. Borella, M. Darche, M. Paques, Paris Eye Imaging group, Hôpital Quinze-Vingts.

Wound healing, actin cable, mean curvature

Source: Ravasio, Almeida et al., Gap geometry dictates epithelial closure efficiency, Nature Communications, 2015.



Wound healing, actin cable, mean curvature

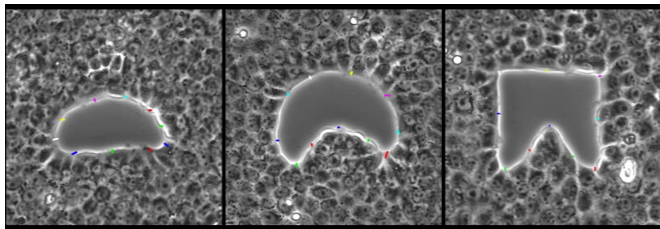


Figure: Closure of in-vitro gaps of different shapes. Life cell imaging of gap closure experiments shown in Fig. 1 B. Tracking over time of randomly chosen point and the edge of the gap are used to illustrate the different speed at different curvatures. Frame rate = 1 frame every 5 minutes.

Source: Ravasio, Almeida et al., *Gap geometry dictates epithelial closure efficiency*, *Nature Communications*, 2015.

What mathematical descriptions?

Can we model the tissue, small lesions, large lesions and their evolution?

Depending on the specific application, we find in the literature:

- Vertex models
- Potts models
- Particle-based models
- Continuum mechanics
- Cahn-Hilliard
- Thresholding scheme (MBO multiphase)
- ...
- Structured model with position and radius

Merriman-Bence-Osher scheme

Given an initial configuration $\mathbf{1}_{C^0} : \mathbb{R}^d \rightarrow \{0, 1\}$,

given a time step $h > 0$,

let G_h be the heat kernel at time $h/2$,

compute $\chi^n = \begin{cases} 1 & \text{where } G_h * \mathbf{1}_{C^{n-1}} > \frac{1}{2}, \\ 0 & \text{otherwise.} \end{cases}$

This is an approximation of the mean curvature flow for the support of χ^0 .

Multiphase thresholding scheme

Given an initial configuration of m cells indexed by i , i.e. a collection of indicator functions $\mathbb{1}_{C_i^0} : \mathbb{R}^d \rightarrow \{0, 1\}$,

given a time step $h > 0$,

let G_h be the heat kernel at time $h/2$,

compute $\psi_i^n = G_h * \mathbb{1}_{C_i^{n-1}}$,

compute $\mathbb{1}_{C_i^n} = \begin{cases} 1 & \text{where } \psi_i^n(x) \geq \max_{j \neq i} \psi_j^n(x), \\ 0 & \text{otherwise.} \end{cases}$

Tim Laux, Felix Otto, Calc. Var. (2016),
Convergence of the thresholding scheme for multi-phase mean-curvature flow

Tim Laux, Theresa M. Simon, CPAM (2018),
Convergence of the Allen-Cahn Equation to Multiphase Mean Curvature Flow

A modified thresholding scheme

$x \in \Omega \subset \mathbb{R}^2$ n iteration number i cell number

$\psi_i(0, x) = \mathbb{1}_{C_i^n}$ initial condition

$\partial_t \psi_i = \Delta \psi_i + \nabla \cdot (\psi_i \nabla V_i)$ drift-diffusion, no-flux b.c.

$V_i = |x - \xi_i(t)|^2$ confinement potential

$\xi_i(0) = \frac{1}{|C_i^n|} \int_{\Omega} \mathbb{1}_{C_i^n} x \, dx$ center of mass

$\frac{d}{dt} \xi_i = -\frac{1}{m} \sum_{j=1}^m \frac{\xi_i - \xi_j}{|\xi_i - \xi_j|} F(|\xi_i - \xi_j|)$ interaction of centers

Work in progress - MBO scheme for epithelia?

Case study 1, closure of small lesions in the epithelium

Working hypotheses:

- small lesions filled via actin cable contraction,
- analogy with wound healing,
- motion by mean curvature at the boundary.

Partial results: agreement with observations, ongoing numerical study.

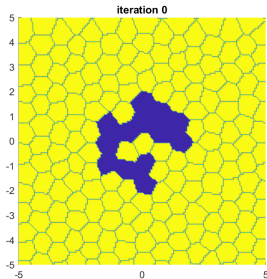
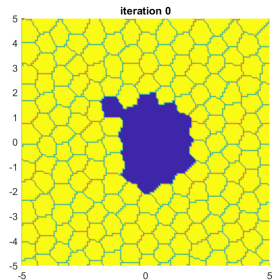
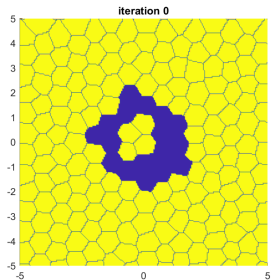
Case study 2, formation of large lesions in the epithelium

Working hypotheses:

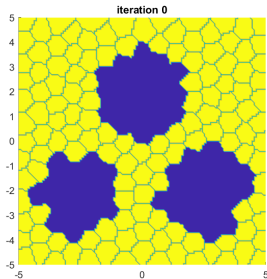
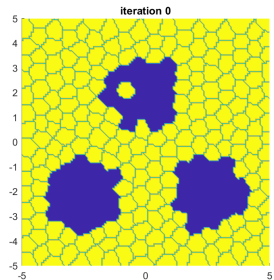
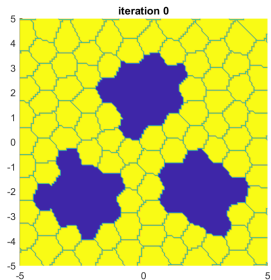
- cells adhere to their neighbours and have a preferred size,
- RPE is subject to a resulting tension;
- larger, senescent cells can't fill gaps effectively, drusen reduces adhesion to the basal membrane.

Partial results: ongoing refinement with adherence, size, tension...

Preliminary simulations I



Preliminary simulations II



THANK YOU FOR YOUR ATTENTION!